DOI: 10.2169/internalmedicine.45.1790

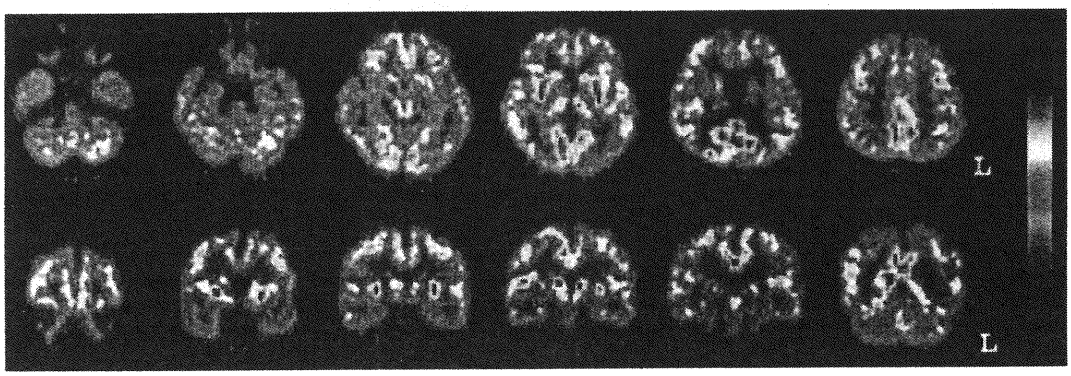

Figure 1. [F-18] FDG PET shows hypometabolism in the frontal and parietal cortices, but metabolism in the striatum is well preserved.

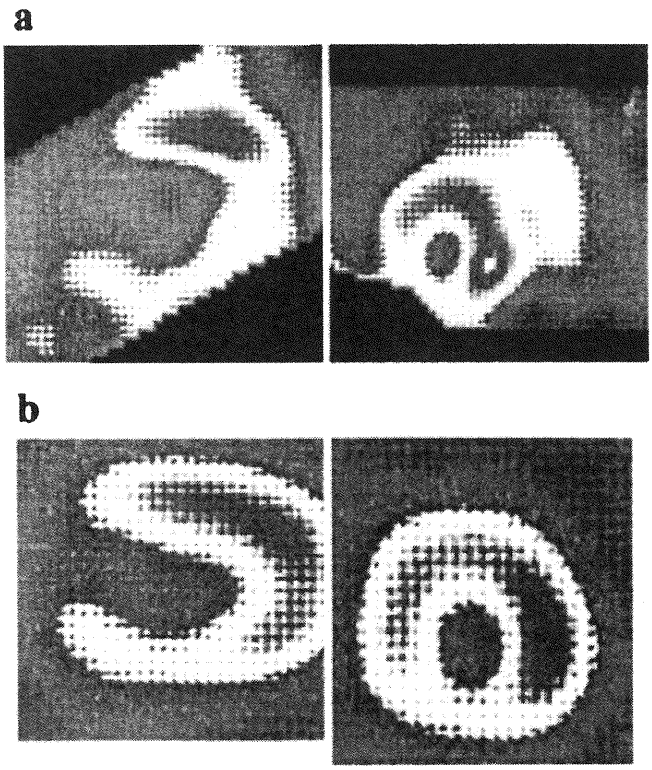

Figure 2. MIBG myocardial SPECT shows persistent low uptake in the infero-posterior area (a); however, [Tc-99m] tetrofosmin SPECT also reveals low uptake inthe sptum and inferior areas (b), suggesting that reduced MIBG uptake is due to cardiac infarction rather than sympathetic denervation. H/M ratio is 1.84.

GBA/metaxin gene has been identified in any form of hereditary parkinsonism, but we do not consider the coexistence of Gaucher's disease and Parkinson's disease to be a mere chance association.

However, the clinical features of Parkinson's disease in type I Gaucher's disease differ somewhat from those of typical Parkinson's disease (1-7). In most published cases, the age at onset of parkinsonism was younger than that seen in typical Parkinson's disease, resting tremor was not evident, and the effect of levodopa was relatively poor. However, further clinical investigations were not described in these articles. In the present case, parkinsonism responded well to levodopa therapy, and [F-18] fluorodeoxyglucose (FDG) PET revealed that function of the striatum, a postsynaptic structure of the nigro-striatal dopaminergic pathway, was well preserved. These findings are identical to those of idiopathic Parkinson's disease.

However, onset as early as the 5th decade of life, absence of resting tremor, and relative preservation of myocardial MIBG uptake are not typical features of idiopathic Parkinson's disease. In particular, MIBG myocardial scintigraphy has been established as a useful tool to distinguish idiopathic Parkinson's disease from other parkinsonian syndromes such as multiple system atrophy and progressive supranuclear palsy. Myocardial uptake of MIBG is completely absent, indicating cardiac sympathetic denervation, in the majority of cases of idiopathic Parkinson's disease, even in the earlier stages, while it is well-preserved in other parkinsonian syndromes (8-11). In the present case, apart from a partial defect of MIBG uptake probably due to old myocardial infarction, MIBG scintigraphy did not indicate a reduced uptake. Normal uptake of MIBG in the present case may represent a lack of Levy body pathology, since MIBG uptake is also preserved in autosomal recessive juvenile parkinsonism with PARK2 anomaly (10).

It is noteworthy that the clinical features of parkinsonism in Gaucher's disease differ distinctly from those of typical Parkinson's disease. While we do not consider the coexistence of Gaucher's disease and Parkinson's disease to represent a mere chance association, it is noteworthy that the clinical features of such cases differ distinctly from those of typical Parkinson's disease. Gaucher's disease-related parkinsonism may account for a small number of cases of Parkinson's disease.

DOI: 10.2169/internalmedicine.45.1790

References

1. Tayebi N, Callahan M, Madike V, et al. Gaucher disease and parkinsonism: a phenotypic and genotypic characterization. Mol Genet Metab **73**: 313-321, 2001.
2. Aharon-Peretz J, Rosenbaum H, Gershoni-Baruch R. Mutations in the glucocerebrosidase gene and Parkinson's disease in Ashkenazi Jews. N Engl J Med **351**: 1972-1977, 2004.
3. Neudorfer O, Giladi N, Elstein D, et al. Occurrence of Parkinson's syndrome in type I Gaucher disease. Q J M **89**: 691-694, 1996.
4. Varkonyi J, Simon Z, Soos K, Poros A. Gaucher disease type I complicated with Parkinson's syndrome. Haematologia **32**: 271-275, 2002.
5. Macaczka M, Rucinska M, Skotnicki AB, Jurczal W. Parkinson's syndrome preceding clinical manifestation of Gaucher's disease. Am J Hematol **61**: 216-217, 1999.
6. McKeran RO, Bradbury P, Taylor D, Stern G. Neurological involvement in type I (adult) Gaucher's disease. J Neurol Neurosurg Psychiatry **48**: 172-175, 1985.
7. Neil JF, Glew RH, Peters SP. Familial psychosis and diverse neurologic abnormalities in adult-onset Gaucher's disease. Arch Neurol **36**: 95-99, 1979.
8. Yoshita M. Differentiation of idiopathic Parkinson's disease from striatonigral degeneration and progressive supranuclear palsy using iodine-123 metaiodobenzylguanidine myocardial scintigraphy. J Neurol Sci **155**: 60-67, 1998.
9. Orimo S, Ozawa E, Nakade S, Sugimoto T, Mizusawa H. ^{123}I-metaiodobenzylguanidine myocardial scintigraphy. J Neurol Neurosurg Psychiatry **67**: 189-194, 1999.
10. Orimo S, Amino T, Yokochi M, et al. Preserved cardiac sympathetic nerve accounts for normal cardiac uptake of MIBG in PARK2. Mov Disord **20**: 1350-1353, 2005.
11. Druschky A, Hilz MJ, Platsch G, et al. Differentiation of Parkinson's disease and multiple system atrophy in early disease by means of I-123-MIBG-SPECT. J Neurol Sci **175**: 3-12, 2000.

脊椎疾患とParkinson病（parkinsonism）*

福武敏夫**

はじめに

Parkinson病（以下，PD）は，よく知られているように，四肢の運動障害を主症状とする神経変性疾患であるが，運動障害以外にも姿勢や肢位異常（特に手指の変形），疼痛（特に腰痛）や骨折などの点で脊椎疾患と深く関連している．いくつかの例を通してその関連および脊椎疾患とPDとの鑑別について解説する．

症例提示

【症例1】

患　者：67歳，男性

既往歴：3年前，上肢巧緻運動障害，排尿障害の精査で歯状突起形成不全と環軸亜脱臼が判明し，千葉大学脳神経外科にて環軸椎後方固定術を受けた．最近不眠などで近医に通院中である．

現病歴：上記術後，散歩可能にまで回復していたが，2～3週前から比較的急に歩きにくくなり，両上肢のしびれ感と巧緻運動障害も出現したため，当院脳神経外科を受診し，精査目的で入院した．頸椎MRIでは髄内高信号所見が認められた（図1a）が，術後の所見と変化なかった．CT脊髄造影でも脊髄圧迫や髄液通過障害は認められなかった（図1b）．神経症状の悪化の原因について当科に相談された．

神経学的所見：

・意識清明で協力的である．後頭部にもやっとした感じがあるという．

・仮面様顔貌がみられ，Myerson徴候が陽性である．

・構音は単調である．

・筋強剛が四肢にみられ，左優位である．

・筋力はおおむね保たれている．

・腱反射は正常範囲である．

・全身，特に両肘から遠位に圧迫されるような嫌なしびれがあり，夜間に増強する（感覚系の診察は省略した）．

・振戦やそのほかの不随意運動はみられない．

・歩行では，軽度前傾姿勢がみられ，左下肢の出が悪く，両側の腕振りが消失している．

印　象：しびれや巧緻運動障害の悪化などには以前の頸髄病変の影響が考えられるが，今回の悪化の主体はparkinsonismと思われた．その原因として，症候のうえからは振戦のないPDも矛盾しないが，悪化の経過が比較的急で，四肢のマーチングの病歴がないなどの点で確定的とは言えなかった．あらためて病歴を取り直すと，近医にてドグマチール® が処方されており，3週前に増量されたことが判明した．このため，もともとPDが潜在し薬物で悪化したか，薬剤性parkinsonismであるかと判断した．

---

* Spinal Disorders and Parkinson's Disease（parkinsonism）

** 亀田メディカルセンター神経内科〔〒296-8602 鴨川市東町929〕，千葉大学医学部／Toshio FUKUTAKE：Department of Neurology, Kameda Medical Center

0914-4412/07/¥400/論文/JCLS

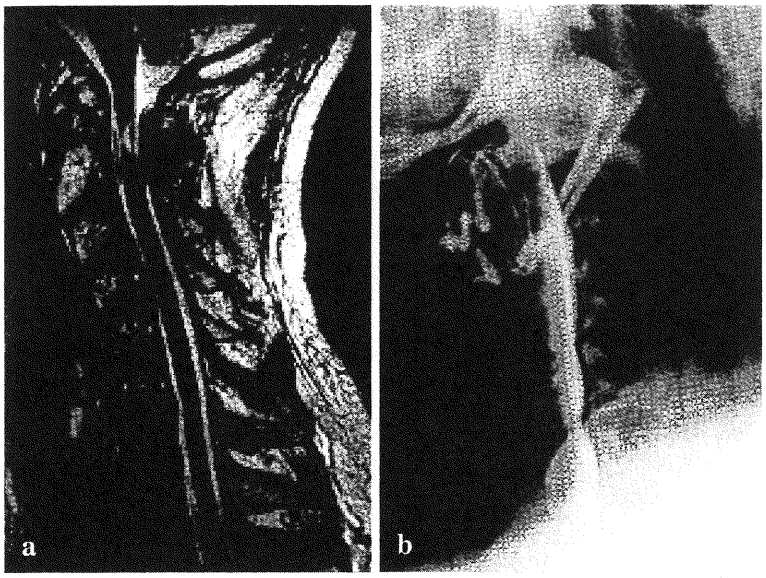

図 1　症例 1 の画像所見
a：頸椎 MRI T 2 強調矢状断像．C_2 高位に髄内高信号域がみられるが，脊髄圧排はない．
b：CT 脊髄造影(C_2 高位)．脊髄圧排や髄液通過障害はない．

経　過：ドグマチール® を中止し，3 週後には筋強剛はごく軽度レベルにまで改善したが，両上肢のしびれが続き，不眠が悪化した．うつ状態と判断され，トリプタノール® 10 mg が開始された．次第に表情が明るくなり，しびれ感も軽減した．

小　括：頸椎手術後に症状が安定していた患者が，3 週くらいの経過で上肢巧緻運動障害としびれ，歩行障害を呈し，薬剤性 parkinsonism と考えられた症例である．

【症例 2】

患　者：80 歳，男性

既往歴：18 年前，前立腺手術．8 年前，事故による右大腿骨骨折と右手首損傷のため，当院整形外科で手術を受けた（その後右殿部痛が残存している）．

現病歴：2 カ月前から腰痛が出現し，右殿部痛も増強した．10 歩の歩行で腰痛が増強し，下腿後面に疼痛が出現するようになり，歩行器を使うようになった．1 カ月前から右示指がつるような感じやしゃべりにくさも出現した．当院整形外科を再診し，間欠性跛行，右傍脊柱筋圧痛が認められた．腰椎単純 X 線検査にて腰部脊柱管狭窄症と診断され，オパルモン® が開始された．しゃべりにくさについて当科受診を勧められ，1 週後に受診した．

神経学的所見：

・意識清明で協力的である．

・軽度の構音障害（不明瞭）が疑われる．

・筋強剛が四肢で疑われる．

・筋力は右手で軽度低下しているが，そのほかは保たれている．

・腱反射は正常範囲であるが，やや活発な印象がある．

・右手掌橈側に表在感覚低下がみられる．

・振戦やそのほかの不随意運動はみられない．

・車いすで入室しており，歩行は診察していない．

印　象：右手の運動・感覚障害は，以前の手首損傷による手根管症候群で説明可能と考えられた．軽度の構音障害と parkinsonism が疑われたため，頭部 CT が撮られたが，正常であった（**図 2 a**）．PD かどうか明確でないため，筆者の外来に紹介された．このときまでに右手指のつる感じやしゃべりにくさは改善していた．診察時，Myerson 徴候は微妙で，四肢に筋強剛が疑われるが，Gegenhalten の可能性があると思われた．歩行ははさみ足歩行であり，総じて PD とは考えられず，頸椎検査の必要があると思われた．

画像検査：大腿部の金属のため，頸椎単純 X 線検査のみ施行し，$C_{4\text{-}6}$ に分節型 OPLL が認められた（**図 2 c**）．

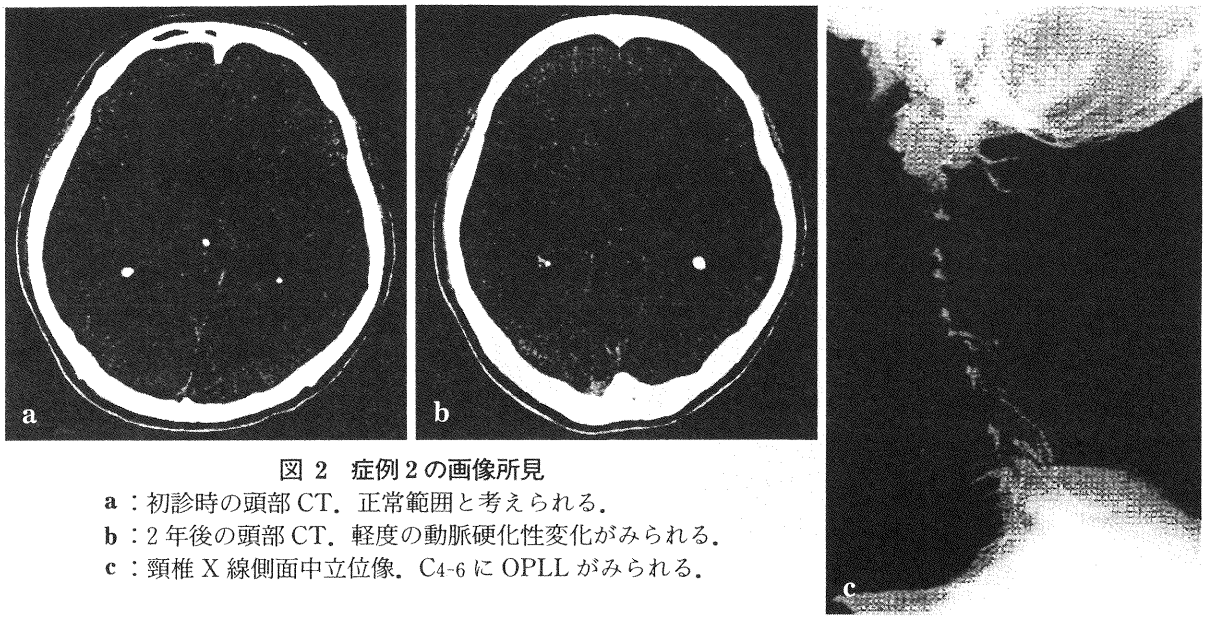

図 2　症例 2 の画像所見
a：初診時の頭部 CT．正常範囲と考えられる．
b：2 年後の頭部 CT．軽度の動脈硬化性変化がみられる．
c：頸椎 X 線側面中立位像．$C_{4\text{-}6}$ に OPLL がみられる．

経　過：整形外科にて，1.5 カ月間頸椎固定を行い，固定中とその後もオパルモン® 服用と歩行訓練を継続し，自宅内では杖歩行可能となった．2 年後，近医神経内科を受診し，軽度の parkinsonism が認められ，頭部 CT が施行された（**図 2 b**）．軽度の全般的萎縮，左内包後脚の淡い低吸収域，内頸動脈の石灰化が認められ，軽度の血管性 parkinsonism と診断された．

小　括：腰部脊柱管狭窄による間欠性跛行の診断時に，しゃべりにくさにより当科に紹介された．軽度の parkinsonism が疑われたが，はさみ足歩行の存在から，OPLL との診断に至り，頸椎固定で歩行障害に改善をみた症例である．2 年後には軽度の血管性 parkinsonism も明らかとなった．

【症例 3】

患　者：68 歳，女性（文献[1]に既報）

既往歴：23 年前，子宮筋腫手術．20 年前，胃潰瘍で胃切除術（その後制酸薬服用）．高血圧症（詳細不明）．20 年前から両上肢の本態性振戦（治療受けず）．

現病歴：10 年前に右手に安静時振戦が加わり，その後同様の振戦が，右下肢，左上肢，左下肢の順に波及した．8 年前から腰痛が慢性化し，歩行障害が進行した．5.5 年前に某医で PD と診断され，治療された．インデラル® で振戦は改善したが，ドーパ合剤で悪化したため，5 年前に鹿島労災病院神経内科を受診した．

初診時神経学的所見：

- 意識清明で協力的である．
- やせ型で亀背がある．
- 仮面様顔貌がある．
- 筋強剛が四肢にみられ，右優位である．
- 安静時，姿勢時の振戦が右優位にみられる．
- 起立歩行姿勢は前傾，前屈が目だち，歩行は小刻みで，後方突進現象がみられる．

印　象：家族歴からも，本態性振戦がもともとあったところに PD が加わったと考えられた．

経　過：アーテン® 6 mg とインデラル® 60 mg で振戦は減弱し，家事が手伝えるようになった．4.5 年前に腰痛が増強し，整形外科にて骨粗鬆症と第 2，第 4 腰椎圧迫骨折を指摘され，薬物治療が開始された．その後，腰痛が軽減し，ドーパ腸溶錠を主とする抗 PD 薬で神経症状が改善するたびに転倒し，順次，第 12 胸椎圧迫骨折，左尺骨茎状突起骨折，左橈骨遠位端骨折，左大腿骨頸部骨折を起こした．

小　括：PD 発症 10 年の経過中に，潜行性の亀背と 2 カ所の腰椎圧迫骨折に加え，転倒により 4 回の四肢・脊椎骨折を起こした高齢女性症例である．

考　察

PDは，振戦，筋強剛，寡動・無動，姿勢反射障害（転倒しやすさ）を主徴とする疾患であり，症例3にみられたN字型ないし逆N字型進展様式も第5の特徴と言える．振戦がしばしば診断の取っ掛かりになるが，振戦がない症例で，運動障害が一側にのみみられる時期には，しばしば脳血管障害と誤診される．また，腰痛をはじめとする疼痛症状の頻度が高く，痛みを訴えて，初めに整形外科を訪れる患者も多い．歩行障害，脊柱の異常（前屈や側弯）や手の肢位の異常（MP関節で屈曲し，PIP・DIP関節で伸展），手の巧緻運動障害も脊椎疾患が疑われる理由になる．

PDと診断するかPDを疑って神経内科に相談するためのポイントは，①筋緊張の特有の亢進〔筋強剛（鉛管様ないし歯車様）〕，②特有の進行様式，③Myerson徴候，④交互反復動作でのすくみ現象などである．小刻み歩行もPDの重要な症状であるが，頸椎症でも出現することに注意が必要である．一見PDと思われる症例が，多発（ラクナ）梗塞と頸椎症であるという経験をしばしばする．このほか，症例1のように薬剤性parkinsonismの症例も多い．もちろん，診断は経験のある神経内科医の仕事であるので，遠慮のない相談が患者のためであろう．

PDは，真の原因は不明であるが，骨量減少やビタミンD欠乏，骨粗鬆症を伴いやすく[2]，高齢者の大腿骨頸部骨折でも脳血管障害と並ぶ危険因子と考えられている．PD患者における腰痛には体幹筋の筋緊張の因子が大きいと思われるが，常に腰椎圧迫骨折も考慮すべきである．症例3のような閉経後の女性患者は特に骨量の減少があると言われる．PDにおいて骨折を増加させている因子として，転倒しやすさや認知・注意障害も重要である．症例3では胃切除の既往も骨量減少にかかわる重要な因子であり，さらに，低酸状態と考えられるのに漫然と長く制酸薬が処方されていたのもCa吸収の点で問題であったと思われる．ちなみに，当初ドーパ合剤で悪化したという病歴も胃切除に伴う薬物吸収異常によると考えられ，腸溶錠を採用した経緯がある．

参考文献

1) 福武敏夫，榊原隆次，森　雅裕：パーキンソン病罹患女性患者にみられた骨折反復の要因の検討．リハ医学 **33**：628-631，1996
2) Sato Y, Kikuyama M, Oizumi K：High prevalence of vitamin D deficiency and reduced bone mass in Parkinson's disease. *Neurology* **49**：1273-1278, 1997

付 2.　　当該年度別刷

（英文のみ）

Available online at www.sciencedirect.com
SCIENCE DIRECT
ELSEVIER
Neuroscience Research 54 (2006) 24–29
Neuroscience Research
www.elsevier.com/locate/neures

Beta-site APP cleaving enzyme 1 (BACE1) is increased in remaining neurons in Alzheimer's disease brains

Hirotsugu Harada [a], Akira Tamaoka [a,*], Kazuhiro Ishii [a], Shin'ichi Shoji [a], Satoshi Kametaka [b], Fuyuki Kametani [c], Yuko Saito [d], Shigeo Murayama [d]

[a] *Department of Neurology, Institute of Clinical Medicine, University of Tsukuba, 1-1-1 Tennodai, Tsukuba, Ibaraki 305-8575, Japan*
[b] *Osaka University, Osaka, Japan*
[c] *Tokyo Institute of Psychiatry, Tokyo, Japan*
[d] *Tokyo Metropolitan Institute of Gerontology, Tokyo, Japan*

Received 19 July 2005; accepted 11 October 2005
Available online 11 November 2005

Abstract

Alzheimer's disease (AD) is characterized by the extensive deposition of amyloid β protein (Aβ) in the brain cortex. Aβ is produced from β-amyloid precursor protein (APP) by β-secretase and γ-secretase. β-Secretase has been identified as beta-site APP cleaving enzyme1 (BACE1). We produced rabbit polyclonal antibodies against the amino and the carboxyl terminals of BACE1. Using these antibodies, BACE1 was characterized in temporal lobe cortices by Western blotting and immunohistochemistry.

Immunohistochemical studies employing anti-GFAP and anti-MAP2 antibodies as well as anti-BACE1 antibodies showed that BACE1 was expressed exclusively in neurons but not in glial cells.

Brain samples were directly extracted by 0.5% SDS and analyzed by Western blotting and densitometer. Although the mean level of BACE1/mg protein in AD brains was not increased, the ratio of BACE1 to MAP2 or to NSE was significantly increased compared with that in control brains.

Taken together, these findings suggest that those neurons that survive in AD brains might generate more BACE1 than normal neurons in control brains, indicating that increased BACE1 activity could be one of the causes of AD. This could justify the development of anti-BACE1 drugs for AD treatment.

Keywords: Alzheimer's disease; Aβ; BACE1

1. Introduction

Alzheimer's disease (AD) is a major form of senile dementia. The appearance of senile plaques with β-amyloid protein (Aβ) as the main component precedes the various pathological changes observed in AD brains (Glenner and Wong, 1984). Aβ is produced by cleavage of Aβ precursor protein (APP) at the amino terminal end by β-secretase and at the carboxyl terminal end by γ-secretase (Hardy and Allsop, 1991). Part of the Aβ released outside the cell is degraded and removed by degradative enzymes; however, increased Aβ production, reduced activity of the degradative enzymes, or reduced activity of the mechanism for removal of Aβ causes the formation of senile plaques through the aggregation and deposition of Aβ (Selkoe, 1999). Furthermore, aggregated Aβ acts against neuronal cells and causes neuronal cell death. It is also said that Aβ activates the phosphorylation of tau protein, causing neurofibrillary degeneration (Rapoport et al., 2002; King, 2005). Therefore, it is considered that inhibition of Aβ production before its deposition, enhancement of Aβ degradation, or clearance of deposited Aβ would be effective in the prevention and treatment of AD. Two phenotypes of BACE have been observed: BACE1 and BACE2. BACE1 is considered to be the major β-secretase because: (1) it exists mainly in the brain, whereas BACE2 is widely distributed throughout the body; (2) only small amounts of BACE2 mRNA have been observed in the brain (Vassar et al., 1999; Bennett et al., 2000; Vassar, 2004). Furthermore, although Aβ production is

* Corresponding author. Fax: +81 29 853 3224.
E-mail addresses: haradah@nona.dti.ne.jp (H. Harada), atamaoka@md.tsukuba.ac.jp (A. Tamaoka).

0168-0102/$ – see front matter
doi:10.1016/j.neures.2005.10.001

increased when human BACE1 is overexpressed in transgenic mice that express a Swedish variant of APP, it is not observed in BACE1 knockout mice (Bodendorf et al., 2002; Luo et al., 2001). These findings suggest that BACE1 inhibitors would suppress the production of Aβ and might be useful as new therapies for AD. To study the localization of BACE1 in AD brains, we prepared anti-human BACE1 antibodies and investigated their reactivity and specificity. We also compared the quantities of BACE1 between normal and AD brains. In addition, we analyzed the relationship between the amount of BACE1 and Aβ species, as measured by enzyme-linked immunosorbent assay (ELISA).

2. Methods

2.1. Case selection

We used frozen temporal lobe cortices (Brodmann area 21) preserved in this hospital and at the Tokyo Metropolitan Institute of Gerontology, including 28 AD cases and 25 normal controls. All AD cases had been diagnosed pathologically according to the criteria of the Reagan Institute Working Group/National Institute on Aging (stages 5 and 6 according to Braak and Braak) (Braak and Braak, 1991; The National Institute on Aging, and Reagan Institute Working Group on Diagnostic Criteria for the Neuropathological Assessment of Alzheimer's Disease, 1997), having been clinically and pathologically differentiated from dementia caused by other diseases. All control subjects had been examined clinically and pathologically. Their causes of death were cerebrovascular infarction or non-neurological diseases. The temporal, frontal, occipital, and parietal lobes from the control brains had been confirmed as pathologically normal for age. No significant differences between AD and control cases were evident concerning distributions of age, gender, or postmortem interval (range, 3–12 h).

2.2. Cultured cells as positive controls expressing human BACE1

pcDNA3-hBACE1 was prepared by cloning full-length BACE1 from the human brain library and then inserting pcDNA3. Next, the construct was transiently forced to express itself in HeLa cells and treated in a lysis buffer (10 mM Tris–HCl [pH 8.0], 150 mM NaCl, 1% NP40, 1% Triton-X100, 2 mM EDTA, protease inhibitor cocktail [Roche, Penzberg, Germany], 1 mM PMSF) on ice for 30 min. The resultant solution was centrifuged at 100 000 × *g* for 15 min to obtain the lysate, the supernatant of this process.

2.3. Preparation of antibodies

Rabbits were immunized with synthetic peptides of the amino terminal (45–55, ETDEEPEEPGR) and the carboxyl terminal (485–501, CLRQQHDDFADDISLLK) of BACE1 to prepare polyclonal antibodies, referred to here as anti-BACE1-N antibody and anti-BACE1-C antibody, respectively.

2.4. Preparation of brain samples and Western blotting

To determine the solubility of BACE1, brain samples were homogenized in a buffer (described below) with three times the volume of the sample, and the whole homogenate was then centrifuged at 100 000 × *g* for 20 min to separate the supernatant. Consecutive extraction was performed with TSE (10 mM Tris–HCl, 150 mM NaCl, 1 mM EDTA), 0.1% Triton-X100/TSE, and 0.5% SDS/TSE, which were added with the inhibitors of proteolytic enzymes (Roche).

The samples of each supernatant and the final pellets were heat-blocked for 10 min in a loading buffer (125 mM Tris–HCl, 20% glycerol, 10% 2-mercaptethanol, 4% SDS, 0.02% bromophenol blue, pH 6.8) and then subjected to electrophoresis on a 10–20% Tris–glycine sodium dodecyl sulfate–polyacrylamide gel (Real Gel Plate, Biocraft, Tokyo, Japan). The samples were then electrically transferred to a transfer membrane (Millipore, Billerico, MA) and blocked for 1 h in phosphate buffered saline (PBS) containing 10% skim milk and 0.1% Tween 20. Anti-BACE1-N antibody (1:2000) and anti-BACE1-C antibody (1:5000) were incubated at 4 °C overnight in a PBS buffer containing 5% bovine albumin. The membrane was rinsed with PBS buffer containing 0.1% Tween 20, incubated with HRP-labeled anti-rabbit IgG (1:5000, Dako-Cytomation, Glostrup, Denmark) for 3 h, and then stained with the detection reagents (Amersham, Buckinghamshire, UK).

Subsequently, direct extraction of a control brain was performed with 0.5% SDS/TSE, which could dissolve more proteins than the other two buffers (TSE or 0.1% Triton-X100/TS), and Western blotting was performed by using 1132-N (1:1000) and 1134-C (1:1000) as authentic BACE1 antibodies against amino acids 45–56 and 487–501, respectively, in addition to anti-BACE1-N antibody (1:2000) and anti-BACE1-C antibody (1:5000).

To study post-translational glycosidation of BACE1, control brain extracts with 0.5% SDS/TSE were incubated at 37 °C for 14 h using an N-Glycosidase F Deglycosylation Kit (Roche), and Western blotting was performed by using anti-BACE1-N antibody and anti-BACE1-C antibody.

To compare total quantities of BACE1, the brains of the 25 normal controls and 28 AD patients were extracted with 0.5% SDS/TSE. After protein amounts were measured by the bicinchoninic acid method (PIERCE, Rockford, IL), concentrations of protein in each sample were adjusted to be equal. Anti-BACE1-C antibody (1:5000), anti-microtubule-associated protein 2 (MAP2) antibody (Sigma, St. Louis, MO), and anti-neuron specific enolase (NSE) antibody (IBL, Gunma, Japan) were used as the primary antibodies, and HRP-labeled anti rabbit antibody was used as the secondary antibody for Western blotting. Measurement and comparison were performed with a densitometer (GS-710, Quantity One, Bio-Rad, Richmond, CA).

2.5. Double immunostaining

Double immunostaining was performed on 6-μm-thick paraffin sections of the temporal lobes from AD brains. After deparaffinization, blocking was performed using PBS containing 5% goat serum and 0.1% Tween 20, then staining was performed with anti-BACE1-C antibody (1:500) as the primary antibody and anti-rabbit IgG (H + L) Fluor 488 (1:400, Molecular Probes Europe BV, Leiden, The Netherlands) as the secondary antibody. Double staining was then performed using anti-MAP2 antibody and anti-GFAP antibody (Progen, Heidelberg, Germany) as the first antibodies and anti-mouse IgG (H + L) Fluor 633 (Molecular Probes Europe BV) as the second antibody. Confocal images were obtained under a confocal laser microscope (TCS SP2, Leica Microsystems, Wetzlar, Germany).

2.6. Quantification of Aβ by sandwich-type enzyme-linked immunosorbent assay (ELISA)

Species of Aβ were measured using the same parts of the temporal lobe cortices that had been used to measure BACE1. Wet tissue (0.5 g) from the cortex of each patient was finely minced, homogenized in 2 ml of 99% formic acid, and centrifuged at 100 000 × *g* for 60 min at 4 °C. The supernatant was neutralized with 1N NaOH, diluted, and subjected to ELISA for Aβ quantitation. To immunochemically identify and quantify different species of Aβ in the cortex, we used a sandwich ELISA with BA27 and BC05, which respectively are HRP-labeled antibodies capable of distinguishing the differing COOH-termini of Aβ 1–40 and 1–42. The sandwich ELISA for Aβ was carried out as described previously (Tamaoka et al., 1995, 1997). Briefly, 100 μl of a standard peptide to establish antibody specificity or a prepared patient sample was placed in a microtiter plate wells previously coated with BNT77, a monoclonal antibody against the NH_2-terminal sequence of Aβ (1–16). Samples were allowed to react at 4 °C for 24 h. After washing with PBS, plates were incubated at 4 °C for 24 h with wells containing HRP-labeled BA27 or BC05, the secondary antibodies for differential measurement of Aβ 40 and Aβ 42, respectively. HRP activities bound to antibodies reacting with samples were assayed with a microtiter plate reader after color development using the TMB microwell peroxidase system (KPL, Gaithersburg, MD).

3. Results

3.1. A 70-kDa protein is detected in the cerebral cortex by anti-BACE1-C antibody and anti-BACE1-N antibody

Supernatants of consecutive extractions from the temporal cortex, final pellets, and positive controls were analyzed on immunoblots with anti-BACE1-C antibody and anti-BACE1-N antibody. Fractions consecutively extracted with TSE, 1% Triton-X100/TSE, and 0.5% SDS/TSE revealed a band migrating at ~70 kDa in all supernatants; however, no band was observed at the same position in the final pellet (Fig. 1a). Since each consecutively extracted fraction contained ~70 kDa protein, Western blotting was performed thereafter on prepared samples obtained by direct extraction of brains with 0.5% SDS/TSE. All these antibodies detected a band migrating at 70 kDa in such fractions (Fig. 1b).

We considered that we had identified mature BACE1, because we observed a band at 70 kDa with both the anti-BACE1-N antibody and the anti-BACE1-C antibody, and it comigrated with a protein with the molecular weight of BACE1, as already reported (Haniu et al., 2000). Deglycosylation of the positive controls with N-glycosidase F resulted in disappearance of the band at 70 kDa and appearance of a band at 50 kDa. Thus, the full-length mature BACE1 was confirmed as the glycosylated form of BACE1 (Fig. 2). Western blotting of control brains with anti-BACE1-C antibody and anti-BACE1-N antibody revealed a band at the same position as the deglycosylated form of BACE1 after treatment with N-glycosidase F.

3.2. BACE1 is expressed mainly in neurons

To determine whether expression of BACE1 in the AD brain occurred mainly in neurons or in astrocytes accompanying the gliosis, we performed double immunostaining of the temporal lobes of AD and normal brains. Stainings of the cortices of the temporal lobe and the hippocampus against anti-BACE1-C antibody were consistent with those for anti-MAP2 antibody. Astrocytes stained for anti-GFAP antibody were not labeled by anti-BACE1-C antibody (Fig. 3). These findings led us to consider that BACE1 was expressed mainly in the neurons, not in glial cells.

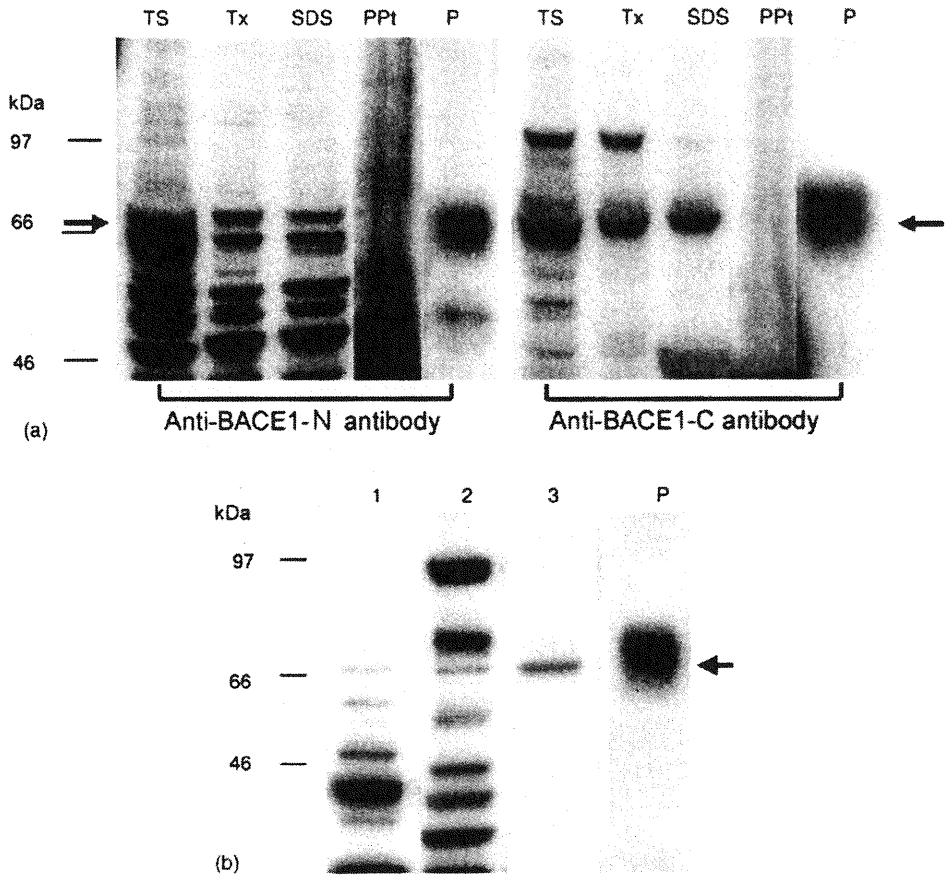

Fig. 1. (a) Immunoblots of sequential extractions of control brain stained with anti-BACE1-N antibody (left) and anti-BACE1-C antibody (right). The acrylamide gel gradient was 10–20%. Lanes: TS, supernatant directly extracted by TSE; Tx, supernatant sequentially extracted by 1% Triton-X100/TSE; SDS, supernatant sequentially extracted by 0.5% SDS/TSE; PPt, final pellet; P, positive control. All brain fractions extracted sequentially by TS, Tx, and SDS were revealed to contain 70 kDa protein (arrow), but PPt did not. (b) Immunoblots of supernatant directly extracted by 0.5% SDS from control brain stained with various anti-BACE1 antibodies. The acrylamide gel gradient was 10–20%. Lanes: 1, 1132-N (1:1000); 2, 1134-C (1:1000); 3, anti-BACE1-N antibody (1:2000); 4, anti-BACE1-C antibody (1:5000); P, positive control stained with anti-BACE1-C antibody. All antibodies detected 70-kDa protein (arrow).

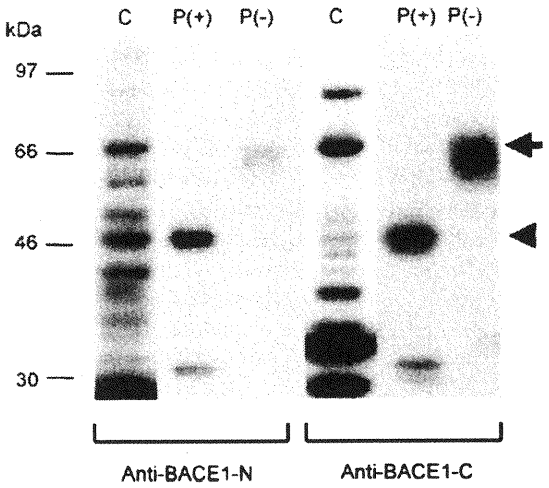

Fig. 2. Immunoblots of recombinant BACE1 (positive control) digested by N-glycosidase F. Lanes; C, supernatant directly extracted by 0.5% SDS from a control brain (untreated); P(+), positive control digested by N-glycosidase F; P(−), untreated positive control. Digestion of positive control by N-glycosidase F altered the molecular weight from 70 (arrow) to 50 kDa (arrowhead), which was consistent with the molecular weight of BACE1 calculated from its amino acid residues. The 70- and 50-kDa bands were also detected in immunoblots of a control brain with anti-BACE1-N antibody (left) and anti-BACE1-C antibody (right).

3.3. BACE1 expression is increased in remaining neurons in AD brains

Because double immunostaining suggested that BACE1 was expressed mainly in neurons, we performed Western blotting with anti-BACE1-C antibody as well as with anti-MAP2 antibody and anti-NSE antibody, measuring the amounts of these proteins (Fig. 4). There were no significant differences in the total amounts of BACE1 between AD and control brains. However, significant decreases in the levels of MAP2 and NSE were observed in the AD group compared with the normal group: the amount of MAP2 in the AD group as a proportion of that in the normal group was 0.29 ($p < 0.05$), and that of NSE was 0.31 ($p < 0.001$). These results were assumed to reflect neuronal loss in the AD brains. The ratios of BACE1 to MAP2 (BACE1/MAP2) and NSE (BACE1/NSE) were 3.0 and 4.6 (both $p < 0.05$), respectively, in the AD group (Fig. 5). We considered that these ratios reflected the relative amounts of BACE1 per neuron. There was a tendency towards an increase in BACE1 concentration with age in both groups, although this trend was not significant. This tendency was greater in AD brains than in the controls (data not shown).

Sandwich ELISA showed that the levels of both Aβ 40 and Aβ 42 were increased in the AD group, as shown previously

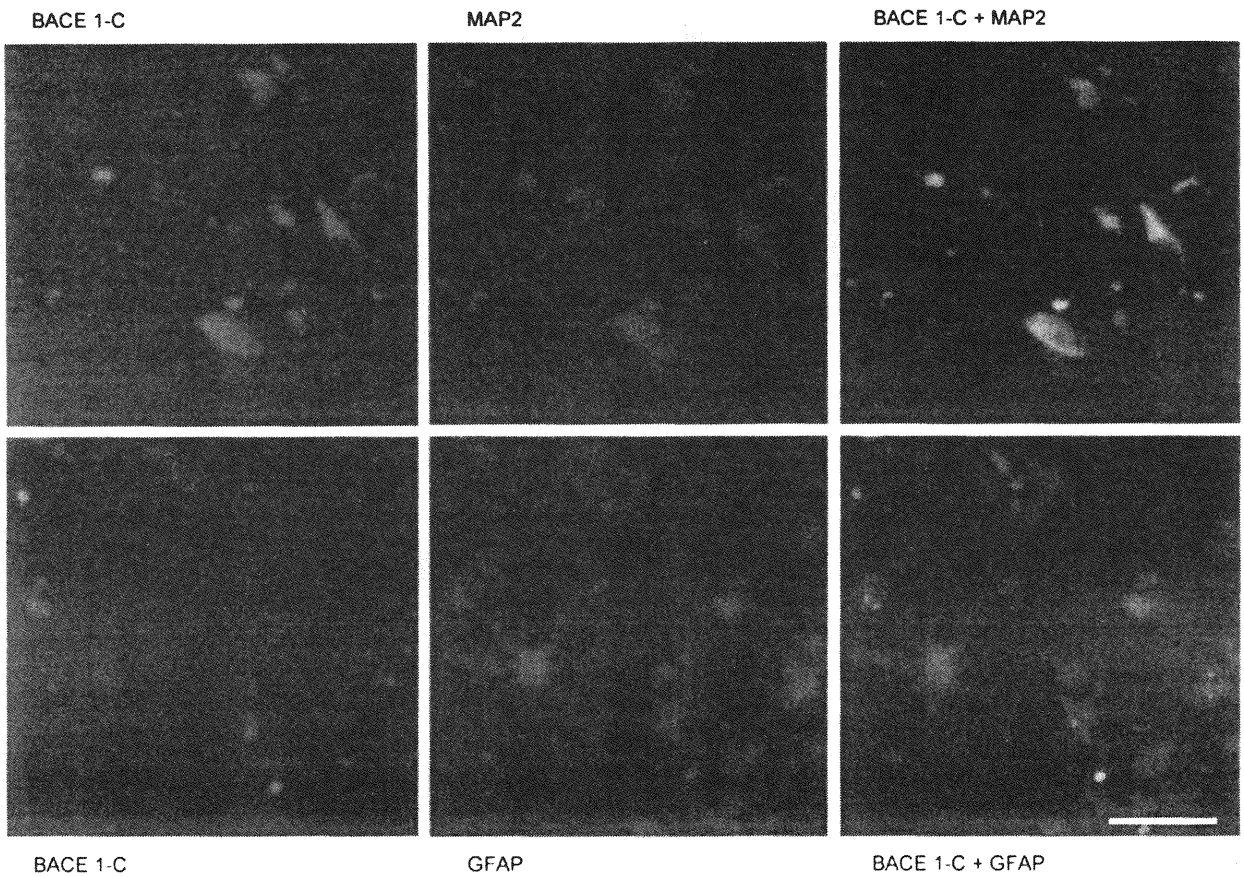

Fig. 3. Immunohistochemical studies of temporal cortex from AD brain, employing anti-MAP2 antibody (upper row, red) and anti-GFAP antibody (lower row, red) as well as anti-BACE1-C antibody (green). BACE1 was expressed exclusively in neurons but not in astrocytes (bar = 40 μm).

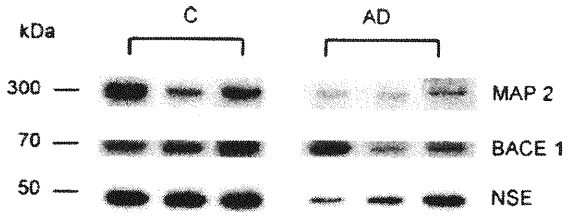

Fig. 4. Western blottings using anti-BACE1-C antibody, anti-MAP2, and anti-NSE in AD and control brains. The samples were extracted with 0.5% SDS/TSE and the concentration of protein in each sample was adjusted to the same level.

(Tamaoka et al., 1995); however, we observed no correlation between the concentrations of BACE1 and Aβ species.

4. Discussion

BACE1 is first synthesized as a transmembrane protein with 501 amino acids. The 1–21 amino acid part of the protein represents a signal peptide and the adjacent 22–45 part represents a proprotein domain. The remaining 46–501 part is considered to undergo maturation through endoplasmic reticulum to become the final 70 kDa mature BACE1 (Vassar et al., 1999; Haniu et al., 2000; Vassar, 2004). Several findings support the identity of the 70-kDa protein recognized by our antibodies as BACE1. (i) In addition to our two antibodies (anti-BACE1-N and anti-BACE1-C), 1132-N and 1134-C, polyclonal antibodies against carboxyl-terminal of BACE1, also detected the same 70-kDa protein band. (ii) Few numbers of extrabands were observed in the Western blottings using anti-BACE1-C antibody in AD and control brains. (iii) Both our novel antibodies against BACE1 immunostained recombinant BACE1 as the band migrating at 70 kDa and deglycosylated recombinant BACE1 at 50 kDa, which is consistent with the molecular weight of BACE1 calculated from its amino acid composition. In the light of the molecular weight of BACE1 calculated by its amino acid composition, with 46–501 amino acid residues, we considered the 50 kDa band that appeared after treatment with N-glycosidase F in the positive controls to be deglycosylated BACE1. The same deglycosylated forms of BACE1 could be identified in normal brains. These findings implied that unmodified BACE1 was present in human brains.

Expression of BACE1 was confirmed by double immunofluorescence staining to occur exclusively in the neurons, as reported previously (Seubert et al., 1993; Zhao et al., 1996). Therefore, we measured the amount of BACE1 protein as well as the amounts of MAP2 and NSE, as neuron-specific proteins, and then examined the ratios of BACE1/MAP2 and BACE1/NSE, which we considered to reflect the level of BACE1 expression per neuron.

We concluded that BACE1 expression per neuron was increased, although the total amount of BACE1 expression in the cortices of the temporal lobe was not increased. This observation implied that Aβ production per neuron might increase before cell death. Fukumoto et al. reported that the total amount of BACE1 protein in the temporal lobes of AD brains tended to increase, as measured by sandwich ELISA using mouse monoclonal anti BACE1 carboxyl terminal antibody and rabbit polyclonal anti BACE1 amino terminal antibody. From the amount of synaptophysin, as measured by ELISA, they also reported that BACE1 expression per neuron was increased in AD brains, because the value of the amount of BACE1 divided by the amount of synaptophysin was increased (Fukumoto et al., 2002). There results are fairly consistent with ours.

Yang et al. reported elevated BACE1 expression and activity in sporadic AD. By using Western blotting analysis they showed that BACE1 levels were significantly higher in the temporal cortex in AD than in non-demented controls. The

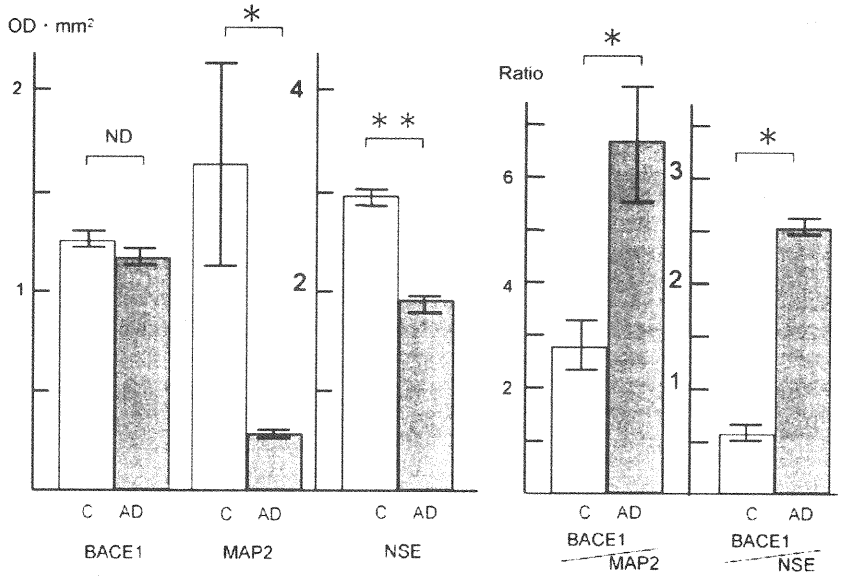

Fig. 5. Protein levels of BACE1, MAP2, and NSE in AD and control (C) brains. The amount of BACE1/mg protein in AD brains was slightly decreased in comparison with that in control brains. However, in AD, the ratios of BACE1 to MAP2 (BACE1/MAP2) and BACE1 to NSE (BACE1/NSE) were significantly increased compared with those in control brains (BACE1/MAP2 and BACE1/NSE $p < 0.05$) ($^{*}p < 0.05$; $^{**}p < 0.0001$).

differences in results between their study and ours could be due to several factors. (i) They used rapidly autopsied brains of AD patients (<3 h), although they did not comment on the postmortem intervals of the non-demented controls. (ii) They normalized BACE1 expression against β-actin. (iii) The AD brain samples that they used might have contained quite large quantities of neurons, as suggested by their levels of MAP-2 and NSE expression. Further studies using brains examined after different postmortem intervals and samples from different brain lesions are needed before we can draw definite conclusions on BACE1 expression (Yang et al., 2003).

Production of Aβ is not seen in BACE1 knockout mice, and no abnormalities are observed in these mice (Luo et al., 2001; Roberds et al., 2001). On the other hand, γ-secretase, which is the cleavage enzyme at the carboxyl terminal side of APP, is also involved in the cleavage of other proteins such as Notch1. Notch1 is an important substance involved in the differentiation and transportation of cells during the embryonic period. It is also known that Notch1 is involved in the differentiation of immune cells in the body, and that inhibition of its cleavage activity causes immune abnormalities (Petit et al., 2001). Therefore, we consider that reduction in the amount of BACE1 is less likely to cause side effects than targeting of γ-secretase.

Several lines of evidence have led to postulation that Aβ accumulation comes from enhancement of its production, promotion of its aggregation, or inhibition of its degradation or excretion (Selkoe, 1999; Hardy and Selkoe, 2002; Iwata et al., 2001). Our results revealed no correlation between the amount of BACE1 protein and the accumulated amount of Aβ species, suggesting that several other factors could cause abnormal accumulation of Aβ in the AD brain. However, BACE1 inhibitors could still provide a new therapy for AD, possibly through inhibition of additional production of Aβ. This is supported by the fact that our study revealed increased production of BACE1 by the surviving neurons in AD brains, and by a previous report that Aβ production is not detected in BACE1 knockout mice.

Acknowledgments

This work was supported in part by Grants-in-Aid to A.T. from the Ministry of Education, Culture, Sports, Science and Technology and from the Ministry of Health, Labour and Welfare.

References

Bennett, B.D., Babu-Khan, S., Loeloff, R., Louis, J.C., Curran, E., Citron, M., Vassar, R., 2000. Expression analysis of BACE2 in brain and peripheral tissues. J. Biol. Chem. 275, 20647–20651.

Bodendorf, U., Danner, S., Fischer, F., Stefani, M., Sturchler-Pierrat, C., Wiederhold, K.H., Staufenbiel, M., Paganetti, P., 2002. Expression of human beta-secretase in the mouse brain increases the steady-state level of beta-amyloid. J. Neurochem. 80, 799–806.

Braak, H., Braak, E., 1991. Neuropathological stageing of Alzheimer-related changes. Acta Neuropathol. (Berlin) 82, 239–259.

Fukumoto, H., Cheung, B.S., Hyman, B.T., Iraozarry, M.C., 2002. β-Secretase protein and activity are increased in the neocortex in Alzheimer disease. Arch. Neurol. 59, 1381–1389.

Glenner, G.G., Wong, C.W., 1984. Alzheimer's disease: initial report of the purification and characterization of a novel cerebrovascular amyloid protein. Biochem. Biophys. Res. Commun. 120, 885–890.

Haniu, M., Denis, P., Young, Y., Mendiaz, E.A., Fuller, J., Hui, J.O., Bennett, B.D., Kahn, S., Ross, S., Burgess, T., Katta, V., Rogers, G., Vassar, R., Citron, M., 2000. Characterization of Alzheimer's beta-secretase protein BACE. A pepsin family member with unusual properties. J. Biol. Chem. 275, 21099–21106.

Hardy, J., Allsop, D., 1991. Amyloid deposition as the central event in the aetiology of Alzheimer's disease. Trends Phamac. 12, 383–388.

Hardy, J., Selkoe, D.J., 2002. The amyloid hypothesis of Alzheimer's disease: progress and problems on the road to therapeutics. Science 297, 353–356.

Iwata, N., Tsubuki, S., Takaki, Y., Shirotani, K., Lu, B., Gerard, N.P., Gerard, C., Hama, E., Lee, H.J., Saido, T.C., 2001. Metabolic regulation of brain Abeta by neprilysin. Science 292, 1550–1552.

King, M.E., 2005. Can tau filaments be both physiologically beneficial and toxic? Biochim. Biophys. Acta 1739, 260–267.

Luo, Y., Bolon, B., Kahn, S., Bennett, B.D., Babu-Khan, S., Denis, P., Fan, W., Kha, H., Zhang, J., Gong, Y., Martin, L., Louis, J.C., Yan, Q., Richards, W.G., Citron, M., Vassar, R., 2001. Mice deficient in BACE1, the Alzheimer's beta-secretase, have normal phenotype and abolished beta-amyloid generation. Nat. Neurosci. 4, H231–H232.

Petit, A., Bihel, F., Alves da Costa, C., Pourquie, O., Checler, F., Kraus, J.L., 2001. New protease inhibitors prevent gamma-secretase-mediated production of Abeta 40/42 without affecting Notch cleavage. Nat. Cell Biol. 3, 507–511.

Rapoport, M., Dawson, H.N., Binder, L.I., Vitek, M.P., Ferreira, A., 2002. Tau is essential to beta-amyloid-induced neurotoxicity. Proc. Natl. Acad. Sci. U.S.A. 99, 6364–6369.

Roberds, S.L., Anderson, J., Basi, G., Bienkowski, M.J., Branstetter, D.G., Chen, K.S., Freedman, S.B., Frigon, N.L., Games, D., Hu, K., Johnson-Wood, K., Kappenman, K.E., Kawabe, T.T., Kola, I., Kuehn, R., Lee, M., Liu, W., Motter, R., Nichols, N.F., Power, M., Robertson, D.W., Schenk, D., Schoor, M., Shopp, G.M., Shuck, M.E., Sinha, S., Svensson, K.A., Tatsuno, G., Tintrup, H., Wijsman, J., Wright, S., McConlogue, L., 2001. BACE knockout mice are healthy despite lacking the primary beta-secretase activity in brain: implications for Alzheimer's disease therapeutics. Hum. Mol. Genet. 10, 1317–1324.

Selkoe, D.J., 1999. Translating cell biology into therapeutic advances in Alzheimer's disease. Nature 399, A23–A31.

Seubert, P., Oltersdorf, T., Lee, M.G., Barbour, R., Blomquist, C., Davis, D.L., Bryant, K., Fritz, L.C., Galasko, D., Thal, L.J., et al., 1993. Secretion of beta-amyloid precursor protein cleaved at the amino terminus of the beta-amyloid peptide. Nature 361, 260–263.

Tamaoka, A., Sawamura, N., Fukushima, T., Shoji, S., Matsubara, E., Shoji, M., Hirai, S., Furiya, Y., Endoh, R., Mori, H., 1997. Amyloid beta protein 42 (43) in cerebrospinal fluid of patients with Alzheimer's disease. J. Neurol. Sci. 148, 41–45.

Tamaoka, A., Sawamura, N., Odaka, A., Suzuki, N., Mizusawa, H., Shoji, S., Mori, H., 1995. Amyloid beta protein 1–42/43 (Abeta 1–42/43) in cerebellar diffuse plaques: enzyme-linked immunosorbent assay and immunocytochemical study. Brain Res. 679, 151–156.

The National Institute on Aging, and Reagan Institute Working Group on Diagnostic Criteria for the Neuropathological Assessment of Alzheimer's Disease, 1997. Consensus recommendations for the postmortem diagnosis of Alzheimer's disease. Neurobiol. Aging 18, S1–S2.

Vassar, R., 2004. BACE1: the beta-secretase enzyme in Alzheimer's disease. J. Mol. Neurosci. 23, 105–114.

Vassar, R., Bennett, B.D., Babu-Khan, S., 1999. β-Secretase cleavage of Alzheimer's amyloid precursor protein by the transmembrane aspartic protease BACE. Science 286, 735–741.

Yang, L.B., Lindholm, K., Yan, R., Citron, M., Xia, W., Yang, X.L., Beach, T., Sue, L., Wong, P., Price, D., Li, R., Shen, Y., 2003. Elevated beta-secretase expression and enzymatic activity detected in sporadic Alzheimer disease. Nat. Med. 9, 3–4.

Zhao, J., Paganini, L., Mucke, L., Gordon, M., Refolo, L., Carman, M., Sinha, S., Oltersdorf, T., Lieberburg, I., McConlogue, L., 1996. Beta-secretase processing of the beta-amyloid precursor protein in transgenic mice is efficient in neurons but inefficient in astrocytes. J. Biol. Chem. 271, 31407–31411.

SHORT REPORT

Selective loss of Purkinje cells in a patient with anti-glutamic acid decarboxylase antibody-associated cerebellar ataxia

Kazuyuki Ishida, Hiroshi Mitoma, Yoshiaki Wada, Teruaki Oka, Junji Shibahara, Yuko Saito, Shigeo Murayama, Hidehiro Mizusawa

J Neurol Neurosurg Psychiatry 2007;**78**:190–192. doi: 10.1136/jnnp.2006.091116

Anti-glutamic acid decarboxylase antibody is associated with the development of progressive cerebellar ataxia and slowly progressive insulin-dependent diabetes mellitus. Previously, the neurophysiological characteristics of IgG in the cerebrospinal fluid of a patient with anti-glutamic acid decarboxylase antibody-associated progressive cerebellar ataxia and slowly progressive insulin-dependent diabetes mellitus were reported. Using a voltage-gated whole-cell recording technique, it was observed that the IgG in the cerebrospinal fluid of the patient selectively suppressed the inhibitory postsynaptic currents in the Purkinje cells. The patient died from aspiration pneumonia. Postmortem examination showed almost complete depletion of the Purkinje cells with Bergmann gliosis. Therefore, the main cause of cerebellar ataxia observed in this case may be attributed to the near-complete depletion of the Purkinje cells. In this paper, the pathomechanisms underlying Purkinje cell damage are discussed.

Glutamic acid decarboxylase (GAD) is a catalytic enzyme that converts glutamic acid to γ-aminobutyric acid, a major inhibitory neurotransmitter. A disease group that is characterised by the presence of a circulating autoantibody against GAD (anti-GAD antibody) includes the following: slowly progressive insulin-dependent diabetes mellitus (SPIDDM), stiff-person syndrome (SPS) and progressive cerebellar ataxia (PCA).[1–3] Anti-GAD antibody is one of the serological diagnostic markers of these diseases. Honnorat *et al*[4] reported a significant link between the anti-GAD antibody and cerebellar ataxia after screening 9000 serum samples. In addition, autoimmune mechanisms against GAD are presumed to be the causative agents of these diseases.[5] Here, we report the autopsy findings of PCA with anti-GAD antibody and discuss the pathomechanism of this rare disease.

CASE REPORT

We previously reported part of the clinical course of a patient with PCA and SPIDDM, and showed the neurophysiological characteristics of IgG in the cerebrospinal fluid.[6] In September 1996, a 66-year-old woman developed cerebellar ataxia of the limbs and trunk. In April 1997, she had sudden onset of hyperglycaemia, and was subsequently diagnosed with anti-GAD-associated SPIDDM. In May 1997, she was bedridden due to severe cerebellar ataxia; other symptoms such as extrapyramidal or pyramidal tracts were not observed. The patient was diagnosed with anti-GAD antibody-associated PCA, and received four rounds of plasma exchange and immunosuppressive treatment. After treatment, the patient showed slight improvement in cerebellar ataxia.

In December 2000, the patient experienced painful spasms and rigidity in the trunk that mimicked symptoms of SPS. Diazepam and baclofen were effective in ameliorating the severe pain associated with the spasms and rigidity. The painful spasms subsided spontaneously within 2 months. The patient died of aspiration pneumonia in October 2001.

During the 5-year clinical course, repeated neuroradiological examinations showed no significant cerebellar atrophy. Using a voltage-gated whole-cell recording technique, we observed that the IgG in the cerebrospinal fluid of the patient, selectively suppressed the inhibitory postsynaptic currents in the Purkinje cells.[6 7]

Postmortem examination

Postmortem examination was performed 22 h after death. The brain weighed 1150 g. The brain and the entire spinal cord were fixed in formalin and prepared for a morphological examination. Macroscopically, there was no atrophy of the cerebrum, brain stem, cerebellum (fig 1A) and spinal cord. The representative areas were examined by routine and immunohistochemical staining, as reported previously.[8] In short, 6-μm thick serial sections were stained with haematoxylin and eosin, Klüver–Barrera and Bodian silver staining. For the immunohistochemical study, 6-μm dewaxed and microwave-irradiated sections were stained using a Ventana 20NX automatic stainer (Ventana, Tucson, Arizona, USA). Microscopical examination showed almost complete depletion of the Purkinje cells and diffuse proliferation of the Bergmann glia (fig 1B). The number of remaining Purkinje cells was no more than one per cerebellar folium. Bodian staining showed multiple empty baskets (fig 1C). There was no specific inflammatory response, and the other structures of the central nervous system, including the cerebral cortex, white matter, basal ganglia, brain stem and spinal cord, did not show marked pathological changes. The pancreas showed a definite and marked decrease in the islets in the tail (fig 1D), and lymphocytic infiltration in the islets situated in the pancreatic body.

DISCUSSION

The selective loss of both Purkinje cells and pancreatic islets was a characteristic finding in this case. The selective degeneration of the Purkinje cells partially mimics the pathological changes observed in paraneoplastic cerebellar ataxia associated with anti-mGluR1 or anti-Yo antibody; however, the exclusive pathological changes related to the Purkinje cells constitute a unique feature of this case.[9 10] On the other hand, the lymphocytic infiltration in the pancreas and the selective decrease in the pancreatic islets corresponded with the pathological findings of autoimmune insulin-dependent diabetes mellitus.[11] Therefore, the main causes of cerebellar ataxia and diabetes mellitus seem to be related to the depletion of the Purkinje cells and the decrease in the pancreatic islets,

Abbreviations: GAD, glutamic acid decarboxylase; PCA, progressive cerebellar ataxia; SPIDDM, slowly progressive insulin-dependent diabetes mellitus; SPS, stiff-person syndrome

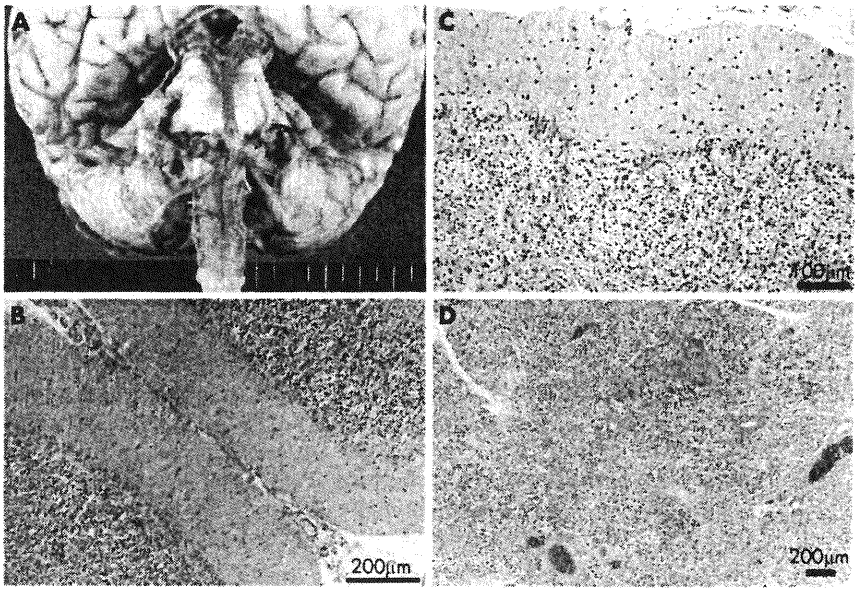

Figure 1 (A) Macroscopic appearance of the brain stem and cerebellum. There are no atrophic changes in the cerebellum and brain stem. (B) Haematoxylin and eosin staining of the cerebellar cortex. There is severe depletion of Purkinje cells and proliferation of Bergmann glia. (C) Bodian staining of the cerebellar cortex. Multiple empty baskets can be observed. (D) Pancreatic tail (haematoxylin and eosin staining). There is a selective decrease in the pancreatic islets.

respectively. To our knowledge, this is the first autopsy report of PCA associated with anti-GAD antibody.

Immunohistochemical staining using anti-GAD and anti-calbindin antibodies failed to react with the patient's specimen; this indicated a complete loss of antigenicity in the patient's specimen, due to postmortem delay and excessive fixation. Therefore, it became difficult to analyse the morphological changes in the other GAD-containing neurones, such as the cerebellar basket cells and the spinal Renshaw cells. However, the existence of multiple empty baskets suggested that, in contrast to the Purkinje cells that were lost, the basket cells were relatively preserved.[12]

We inferred two possible pathomechanisms to explain the Purkinje cell damage: indirect and direct immune-mediated mechanisms. The indirect mechanism might be associated with excitotoxicity of the Purkinje cells by the selective suppression of inhibitory postsynaptic currents and the attenuation of inhibition of excitatory postsynaptic currents by the anti-GAD antibody.[6 7 13] The direct mechanism might be mediated by cytotoxic reactions against the Purkinje cells caused by the invading leucocytes, as observed in the pancreatic islets. However, it is presently unclear whether the mechanisms that are more likely to have caused the Purkinje cell damage are indirectly or directly immune-mediated.

The patient experienced painful muscle spasms that mimic symptoms of SPS. The muscle spasms observed in SPS are considered to occur as a result of the dysfunction of the Renshaw cells that are γ-aminobutyric acid inhibitory interneurones in the spinal cord.[14] Various pathological changes are observed in the spinal cord of patients with SPS; however, lymphocytic cuffing and a decrease in the number of anterior horn neurones are considered to be representative of SPS.[15] In contrast, the pathological changes observed in our patient were unremarkable; this suggests that the Renshaw cells were not severely damaged. This may explain the transient nature of the muscular spasms in this case.

Based on the quantitative analysis of the brain autopsy of a patient with SPS and without cerebellar ataxia, Warich-Kirches *et al*[16] reported diminished cell density of the inhibitory neurones in the cerebellar cortex. Combining their case results with ours might show the phenotypic overlap of the anti-GAD autoimmunity-associated neurological diseases.

Authors' affiliations
Kazuyuki Ishida*, Department of Neurology, Tamagawa Hospital, Setagaya-ku, Tokyo, Japan
Hiroshi Mitoma, Mitoma Neurological Clinic, Shinjuku-ku, Tokyo, Japan
Yoshiaki Wada, Department of Rehabilitation, Tamagawa Hospital, Setagaya-ku, Tokyo, Japan
Teruaki Oka, Department of Pathology, Kanto Central Hospital, Setagaya-ku, Tokyo, Japan
Junji Shibahara, Department of Pathology, University of Tokyo, Bunkyo-ku, Tokyo, Japan
Yuko Saito, Shigeo Murayama, Department of Neuropathology, Tokyo Metropolitan Institute of Gerontology, Itabashi-ku, Tokyo, Japan
Hidehiro Mizusawa, Department of Neurology and Neurological Science, Tokyo Medical and Dental University Graduate School, Bunkyo-ku, Tokyo, Japan

Competing interests: None declared.

Informed consent was obtained from the family of the patient for the publication of her details in this paper.

Correspondence to: Dr Kazuyuki Ishida, Institute of Oriental Medicine, Tokyo Women's Medical University, School of Medicine, 4th floor, Shinjuku NS Building, 2-4-1 Nishi-Shinjuku, Shinjuku-ku, Tokyo 163-0804, Japan; k-ishida@iom.twmu.ac.jp

Received 17 February 2006
Revised 13 October 2006
Accepted 25 October 2006
Published Online First 17 November 2006

REFERENCES

1 **Seissler J**, Amann J, Mauch L, *et al*. Prevalence of autoantibodies to the 65- and 67-kD isoforms of glutamate decarboxylase in insulin-dependent diabetes mellitus. *J Clin Invest* 1993;**92**:1394–9.
2 **Saiz A**, Arpa J, Sagasta A, *et al*. Autoantibodies to glutamic acid decarboxylase in three patients with cerebellar ataxia, late-onset insulin-dependent diabetes mellitus, and polyendocrine autoimmunity. *Neurology* 1997;**49**:1026–30.
3 **Vianello M**, Tavolato B, Giometto B. Glutamic acid decarboxylase autoantibodies and neurological disorders. *Neurol Sci* 2002;**23**:145–51.
4 **Honnorat J**, Saiz A, Giometto B, *et al*. Cerebellar ataxia with anti-glutamic acid decarboxylase antibodies: study of 14 patients. *Arch Neurol* 2001;**58**:225–30.
5 **Dalakas MC**, Li M, Fujii M, *et al*. Stiff person syndrome: quantification, specificity, and intrathecal synthesis of GAD65 antibodies. *Neurology* 2001;**57**:780–4.
6 **Ishida K**, Mitoma H, Song SY, *et al*. Selective suppression of cerebellar GABAergic transmission by an autoantibody to glutamic acid decarboxylase. *Ann Neurol* 1999;**46**:263–7.

7 **Mitoma H**, Song SY, Ishida K, *et al*. Presynaptic impairment of cerebellar inhibitory synapses by an autoantibody to glutamate decarboxylase. *J Neurol Sci* 2000;**175**:40–4.
8 **Saito Y**, Suzuki K, Nanba E, *et al*. Niemann-Pick type C disease: accelerated neurofibrillary tangle formation and amyloid beta deposition associated with ApoE e4 homozygosity. *Ann Neurol* 2002;**52**:351–5.
9 **Coesmans M**, Smitt PA, Linden DJ, *et al*. Mechanisms underlying cerebellar motor deficits due to mGluR1-autoantibodies. *Ann Neurol* 2003;**53**:325–36.
10 **Verschuuren J**, Chuang L, Rosenblum MK, *et al*. Inflammatory infiltrates and complete absence of Purkinje cells in anti-Yo-associated paraneoplastic cerebellar degeneration. *Acta Neuropathol (Berl)* 1996;**91**:519–25.
11 **Nakanishi K**, Kobayashi T, Miyashita H, *et al*. Relationships among residual beta cells, exocrine pancreas, and islet cell antibodies in insulin-dependent diabetes mellitus. *Metabolism* 1993;**42**:196–203.
12 **Gatti RA**, Vinters HV. Cerebellar pathology in ataxia-telangiectasia: the significance of basket cells. *Kroc Found Ser* 1985;**19**:225–32.
13 **Mitoma H**, Ishida K, Shizuka-Ikeda M, *et al*. Dual impairment of GABAA- and GABAB-receptor-mediated synaptic responses by autoantibodies to glutamic acid decarboxylase. *J Neurol Sci* 2003;**208**:51–6.
14 **Meinck HM**, Ricker K, Hulser PJ, *et al*. Stiff man syndrome: clinical and laboratory findings in eight patients. *J Neurol* 1994;**241**:157–66.
15 **Warren JD**, Scott G, Blumbergs PC, *et al*. Pathological evidence of encephalomyelitis in the stiff man syndrome with anti-GAD antibodies. *J Clin Neurosci* 2002;**9**:328–9.
16 **Warich-Kirches M**, Von Bossanyi P, Treuheit T, *et al*. Stiff-man syndrome: possible autoimmune etiology targeted against GABA-ergic cells. *Clin Neuropathol* 1997;**16**:214–19.

Acta Neuropathol (2006) 111: 329–340
DOI 10.1007/s00401-006-0048-x

ORIGINAL PAPER

**Rohan de Silva · Tammaryn Lashley
Catherine Strand · Anna-Maria Shiarli
Jing Shi · Jinzhou Tian · Kathryn L. Bailey
Peter Davies · Eileen H. Bigio · Kunimasa Arima
Eizo Iseki · Shigeo Murayama · Hans Kretzschmar
Manuela Neumann · Carol Lippa · Glenda Halliday
James MacKenzie · Rivka Ravid · Dennis Dickson
Zbigniew Wszolek · Takeshi Iwatsubo
Stuart M. Pickering-Brown · Janice Holton
Andrew Lees · Tamas Revesz · David M. A. Mann**

An immunohistochemical study of cases of sporadic and inherited frontotemporal lobar degeneration using 3R- and 4R-specific tau monoclonal antibodies

Received: 2 December 2005 / Revised: 20 January 2006 / Accepted: 21 January 2006 / Published online: 22 March 2006

Abstract The pathological distinctions between the various clinical and pathological manifestations of frontotemporal lobar degeneration (FTLD) remain unclear. Using monoclonal antibodies specific for 3- and 4-repeat isoforms of the microtubule associated protein, tau (3R- and 4R-tau), we have performed an

R. de Silva · A. Lees
Reta Lila Weston Institute of Neurological Studies,
University College London, Windeyer Building,
46 Cleveland St, W1T 4JF, London, UK

T. Lashley · C. Strand · J. Holton · T. Revesz
Department of Molecular Neuroscience,
Queen Square Brain Bank, Institute of Neurology,
University College London, Queen Square,
WC1N 3BG, London, UK

A.-M. Shiarli · J. Shi · J. Tian · K. L. Bailey
S. M. Pickering-Brown · D. M. A. Mann (✉)
Centre for Clinical Neurosciences, University of Manchester,
Greater Manchester Neurosciences Centre, Hope Hospital,
M6 8HD, Salford, UK
E-mail: david.mann@manchester.ac.uk
Tel.: +44-161-2062580
Fax: +44-161-2060388

J. Shi · J. Tian
Department of Care of the Elderly,
Dongzhimen Hospital,
100700, Beijing, P R China

P. Davies
Department of Pathology, Albert Einstein College of Medicine,
Bronx, NY, 10461, USA

E. H. Bigio
Northwestern University Alzheimer's Disease Center,
Chicago, IL, 60611, USA

K. Arima
National Centre of Neurology and Psychiatry,
Musashi Hospital, 187-8551, Tokyo, Japan

E. Iseki
Juntendo Tokyo Koto Geriatric Medical Center,
Juntendo University School of Medicine, 136-0075, Tokyo, Japan

S. Murayama
Department of Neuropathology, Tokyo Metropolitan
Institute of Gerontology, 173, Tokyo, Japan

H. Kretzschmar · M. Neumann
Reference Centre for Prion Diseases and Neurodegenerative
Diseases, Institute of Neuropathology, Marchioninistr. 17,
81377, Munchen, Germany

C. Lippa
Memory Disorders Centre, Drexel University College of Medicine,
Philadelphia, PA, 10129, USA

G. Halliday
Department of Neuropathology,
Prince of Wales Medical Research Institute,
University of New South Wales, NSW 2031, Randwick, Australia

J. MacKenzie
The Royal Infirmary, Foresterhill, AB25 2ZD, Aberdeen, Scotland

R. Ravid
Netherlands Brain Bank, Meibergdreef 33,
1105 AZ, The Netherlands

D. Dickson · Z. Wszolek · S. M. Pickering-Brown
Mayo Clinic, 4500 San Pablo Rd,
Jacksonville, FL, 32224, USA

T. Iwatsubo
Department of Neuropathology and Neuroscience,
University of Tokyo, 113-0033, Tokyo, Japan

immunohistochemical study of the tau pathology present in 14 cases of sporadic forms of FTLD, 12 cases with Pick bodies and two cases without and in 27 cases of familial FTLD associated with 12 different mutations in the tau gene (*MAPT*), five cases with Pick bodies and 22 cases without. In all 12 cases of sporadic FTLD where Pick bodies were present, these contained only 3R-tau isoforms. Clinically, ten of these cases had frontotemporal dementia and two had progressive apraxia. Only 3R-tau isoforms were present in Pick bodies in those patients with familial FTLD associated with L266V, Q336R, E342V, K369I or G389R *MAPT* mutations. Patients with familial FTLD associated with exon 10 N279K, N296H or +16 splice site mutations showed tau pathology characterised by neuronal neurofibrillary tangles (NFT) and glial cell tangles that contained only 4R-tau isoforms, as did the NFT in P301L *MAPT* mutation. With the R406W mutation, NFT contained both 3R- and 4R-tau isoforms. We also observed two patients with sporadic FTLD, but without Pick bodies, in whom the tau pathology comprised only of 4R-tau isoforms. We have therefore shown by immunohistochemistry that different specific tau isoform compositions underlie the various kinds of tau pathology present in sporadic and familial FTLD. The use of such tau isoform specific antibodies may refine pathological criteria underpinning FTLD.

Introduction

Frontotemporal lobar degeneration (FTLD) describes a clinically and pathologically heterogeneous group of forms of dementia that have onset of illness usually between ages of 35 and 75 years and affect males and females equally [41, 56]. A previous family history of a similar disorder occurs in about half of patients [41, 53, 56] and in many such familial cases a mutation in the gene encoding the microtubule associated protein, tau (*MAPT*) on chromosome 17 seems causal (see Ref. [15, 32] for recent reviews). To date, about 35 causal *MAPT* mutations in around 150 families have been identified and the term frontotemporal dementia with parkinsonism linked to chromosome 17 (FTDP-17) was adopted [12] to accommodate the clinical and genetic features of such cases. At autopsy, patients with FTLD generally show atrophy of the frontal and temporal lobes of the brain associated with a degeneration and loss of large pyramidal neurons from such regions irrespective of clinical subtype or family history [41, 56]. However, under this umbrella of pathological change, histopathological differences occur [41, 55, 62] and over the years there have been several attempts at classification based upon microscopic appearances.

In the first case reports, made over a century ago by Arnold Pick, the characterising features of intraneuronal argyrophilic inclusions (Pick bodies) and swollen or ballooned neurons (Pick cells) were described and the eponym Pick's disease was coined to distinguish such cases from those of Alzheimer's disease where senile plaques and neurofibrillary tangles were the key pathology. However, recognizing that clinically similar forms of FTLD occurred without such Pick- or Alzheimer-type changes being present led to the scheme by Constantinidis [7] in which three variants of FTLD were identified: one with Pick bodies and Pick cells (type A), one with only Pick cells (type B) and one with neither (type C). Later immunohistochemical studies [33] indicated either a Pick-type of histology based on the presence of tau-positive Pick bodies (equivalent to Constantinidis type A) or a microvacuolar-type histology in which no tau intraneuronal inclusions (Pick bodies) were seen (equivalent to Constantinidis types B and C). Recent surveys [22, 31, 37, 41, 55, 62] indicate that about half of cases of FTLD show a histopathology based on the accumulation of insoluble aggregates of tau protein within neurons and glial cells of the cerebral cortex and hippocampus. In most other cases, termed FTLD-U, tau negative but ubiquitin positive inclusions usually occur within cerebral cortex and hippocampus and when clinical motor neuron disease (MND) is also present the term FTLD-MND can be ascribed. Sometimes, neither tau nor ubiquitin inclusions are seen; such cases have been labelled as dementia lacking distinctive histology. These observations are broadly in line with the recommendations of a consensus conference held in 2001 in an attempt to establish internationally accepted clinical and neuropathological criteria for FTLD [34]. Nonetheless, at the time such criteria were put forward it was recognized that they were likely to be interim and subject to review in the light of expanding knowledge of this disorder—a point reiterated in some most recent surveys [37, 55]

Tau-based pathology in FTLD can occur in either sporadic or familial cases. In sporadic cases of FTLD, tau pathology usually takes the form of Pick bodies and Pick cells, though in such cases some tau positive glial cells and dystrophic neurites can often be seen [66], though if cases of corticobasal degeneration (CBD), progressive supranuclear palsy (PSP) or argyrophilic grain disease are included under the rubric of FTLD as has been the case in certain recent surveys [22, 31, 37] a neurofibrillary tangle-based tau pathology becomes more common.

In some familial cases (i.e., those with FTDP-17) with missense mutations within coding regions of exons 1, 9, 11, 12 and 13 of *MAPT* there are swollen nerve cells and rounded neuronal inclusions within large and small pyramidal neurones of the cerebral cortex and pyramidal and granule cells of the hippocampus reminiscent of the Pick bodies seen in sporadic disease [4, 14, 23, 29, 30, 39, 42, 45, 47, 50, 52]. Such mutations affect all six isoforms of tau, generating mutated tau molecules that (variably) lose their ability to interact with microtubules [20, 21, 23, 39, 42, 50, 51], increasing their propensity to self-aggregate into fibrils [20, 21, 23, 42, 47, 51]. Other *MAPT* mutations cluster around, or

lie within a predicted regulatory stem loop structure of a splice acceptor domain of *MAPT* pre-mRNA that determines the inclusion or exclusion of exon 10 by alternative splicing during gene transcription [2, 3, 5, 6, 9, 11, 17, 19, 20, 24, 25, 35, 40, 43, 46, 48, 52, 58–60], destabilizing the stem loop [24, 58] or strengthening [11, 18, 20] or destroying [11] splice enhancing, or splice silencing [11, 59] elements in the 5′ region of exon 10. Such cases show insoluble aggregated tau deposits as neurofibrillary tangle-like structures within large and smaller pyramidal cells of cortical layers III and V and prominently within glial cells in the deep white matter, globus pallidus and internal capsule [2, 17, 19, 35, 43, 46, 51, 58–60]. However, other exon 10 mutations do not affect the splicing of exon 10 [11, 24] but induce conformational changes in tau molecules containing exon 10 that interfere with microtubule function and lead to aggregation of the mutated tau into neurofibrillary tangles [18, 36, 59].

Although the brain tau isoform composition has been extensively analysed by western blotting both in cases of sporadic FTLD where Pick bodies [1, 8, 37, 53, 61, 65] or Pick-like bodies [37] are present and in many of the cases with FTDP-17 [2–6, 9, 14, 17, 19, 23, 25, 29, 30, 35, 36, 39, 42, 43, 45–47, 50, 52, 59, 60, 62, 65], certain ambiguities remain. For example, in cases of sporadic FTLD where Pick bodies are seen in histology, most western blotting studies have detected only tau isoforms with 3-repeat microtubule binding domains (3R-tau) [8, 37, 54], though other investigations have shown certain cases to show tau isoforms with both 3R-tau and 4-repeat microtubule binding domains (4R-tau) [1, 37, 62, 66] and in yet others only 4R-tau is seen [37, 62, 66]. Such disparities have led to controversies as to whether Pick bodies are composed of only 3R-tau, only 4R-tau or an admixture of 3R- and 4R-tau isoforms. Similarly, in some cases of FTDP-17 with Pick bodies (e.g., K257T *MAPT* mutation Ref. [50]) western blotting has likewise shown only 3R-tau to be present, whereas in other cases (e.g., L266V, G272V, G342V and G389R *MAPT* mutations) both 3R-tau and 4R-tau isoforms are seen [4, 14, 23, 31, 45]. One possible explanation for these apparent inconsistencies may lie in differing anatomical compartmentalizations of 3R- and 4R- tau isoforms between cases, a distinction that is lost upon the tissue homogenization required for western blotting. Specific immunohistological patterns associated with 3R- and 4R-tau isoforms cannot be distinguished using phospho-dependent and phospho-independent tau antibodies that recognize tau epitopes shared by all six tau isoforms.

In the present study, therefore, we have investigated in situ, using monoclonal antibodies specific for 3R- and 4R-tau isoform species, the isoform composition of the tau histopathological changes in 14 cases of sporadic FTLD and 27 cases of familial FTLD associated with 11 different mutations in *MAPT*, for which tau isoform patterns on western blotting have already been reported, in order to reconcile such inconsistencies and to provide further insight into disease classification by the use of tau antibodies not available when the last pathological criteria [34] were proposed.

Materials and methods

Brain tissues from 14 cases with sporadic FTLD (cases #1–14), in 12 of whom (cases #1–12) previous pathological investigations had shown Pick bodies to be present and five cases of familial FTLD (cases #30–34) with exon 10 +16 *MAPT* mutation were obtained from the Manchester Brain Bank. Seven of the sporadic FTLD cases (cases #1, 2, 4–7 and 13) had been included (as cases # 4–8, 10 and 12, respectively) in a previous study [66] investigating tau isoform composition in a series of 14 cases of FTLD. Eight of the sporadic FTLD cases (cases #1, 2, 4–7, 9 and 13) had been included (as cases #10, 11, 12, 13, 14, 15, 17 and 16, respectively) in a previous study of ours [62] also investigating tau isoform composition in FTLD. Tissues from the other 22 familial FTLD cases with *MAPT* mutations were kindly supplied in collaboration by colleagues from different centres across the world. Selected clinical and pathological details for all cases are given in Table 1. Full clinical and pathological descriptions for 25 of the 27 cases with *MAPT* mutations have been previously reported by the originating authors (see Table 1 for details of citation); the other two cases remain unreported to date.

Serial sections were cut at a thickness of 6 μm from formalin-fixed, wax-embedded blocks of frontal cortex (BA 8/9) from all 14 sporadic FTLD cases and 27 familial FTLD cases with *MAPT* mutations and from temporal cortex (BA 21/22) to include the hippocampus in the 14 sporadic FTLD cases alone and mounted onto APES-coated slides. One set of sections was immunostained for insoluble pathological tau proteins by a standard immunoperoxidase method using the phospho-dependent tau antibody AT8 (1:750) (Innogenetics, Belgium). AT8 antibody is raised against the phosphorylated Ser 202/Thr 205 epitope and immunoreacts with PHF-tau in AD [16]. It will detect all isoforms of tau in which this epitope is phosphorylated. Other sets of sections were stained with the 3R-tau specific monoclonal antibody RD3 [10] (1:3000; Upstate, Dundee, UK) and the 4R-tau specific monoclonal antibody ET3 (gift of P Davies, 1:100) as described [10]. Briefly, sections were deparaffinised in xylene and rehydrated in decreasing concentrations of alcohol. Endogenous peroxidase activity was blocked with 0.3% H_2O_2 in methanol for 10 min. Sections were pressure cooked for 10 min in 0.01 M citrate buffer pH6.0. Sections were incubated in 10% non-fat milk to block non-specific staining, then with the primary antibodies RD3 and ET3 for 1 h at room temperature. This was followed by several washes in PBS and treatment with biotinylated

Table 1 Selected clinical and pathological details

Case	Pathology	*MAPT* mutation	Gender	Onset (years)	Death (years)	Duration (years)	APOE genotype	Brain weight (g)
1 [55, 62]	Pick bodies	None	F	53	60	7	3.3	960
2 [55, 62]	Pick bodies	None	M	46	56	10	3.3	1,150
3 [55, 62]	Pick bodies	None	M	54	63	9	n.a.	n.a.
4 [55, 62]	Pick bodies	None	F	52	62	10	3.4	928
5 [55, 62]	Pick bodies	None	F	76	84	8	3.3	1,235
6 [55, 62]	Pick bodies	None	F	50	58	8	2.2	1,065
7 [55, 62]	Pick bodies	None	M	63	74	11	2.3	990
8 [55, 62]	Pick bodies	None	M	73	77	4	3.3	n.a.
9 [55, 62]	Pick bodies	None	M	47	61	14	3.4	980
10 [55, 62]	Pick bodies	None	M	59	69	10	3.3	885
11 [55, 62]	Pick bodies	None	M	55	67	12	3.3	895
12 [55, 62]	Pick bodies	None	F	51	57	6	3.3	1,210
13 [55, 62]	NFT-like	None	F	57	64	7	3.3	1,000
14 [55, 62]	NFT-like	None	F	64	70	6	3.3	1,090
15 [23]	Pick bodies	L266V	M	32	36	3.5	n.a.	1,050
16 [2]	NFT, glial tangles	N279K	M	46	57	11	3.3	1,250
17 [2]	NFT, glial tangles	N279K	M	44	50	6	3.3	1,420
18 [6, 64]	NFT, glial tangles	N279K	M	44	50	6	3.4	1,290
19 [6, 64]	NFT, glial tangles	N279K	F	45	48	3	3.3	1,100
20 [6, 64]	NFT, glial tangles	N279K	M	56	58	2	2.3	1,400
21 [6, 64]	NFT, glial tangles	N279K	F	45	53	8	2.4	1,000
22 [6, 64]	NFT, glial tangles	N279K	M	57	63	6	3.4	1,100
23 [6, 64]	NFT, glial tangles	N279K	M	41	52	11	2.3	1,100
24 [25]	NFT, glial tangles	N296H	M	57	62	3	3.3	960
25 [51, 63]	NFT	P301L	M	~48	60	>12	3.3	1,331
26 [51, 63]	NFT	P301L	M	44	52	8	2.3	1,087
27 [51, 63]	NFT	P301L	F	54	76	22	2.2	1,006
28 [51, 63]	NFT	P301L	F	59	64	5	3.3	1,013
29 [19, 60]	NFT, glial tangles	S305S	F	48	51	3	n.a.	1,053
30 [46]	NFT, glial tangles	Exon 10 +16	M	50	61	11	3.4	1,016
31 [46]	NFT, glial tangles	Exon 10 +16	F	46	58	12	3.3	996
32 [46]	NFT, glial tangles	Exon 10 +16	M	43	55	12	3.4	1240
33 [46]	NFT, glial tangles	Exon 10 +16	F	52	65	13	2.3	1,040
34 [46]	NFT, glial tangles	Exon 10 +16	F	48	56	8	3.4	1,175
35[uc]	NFT, glial tangles	Exon 10 +16	M	57	63	6	3.3	1,440
36 [47]	Pick bodies	Q336R	M	58	68	10	3.3	1,102
37 [30]	Pick bodies	E342V	F	48	55	7	3.3	1,020
38 [42]	Pick bodies	K369I	F	52	61	9	n.a.	885
39[uc]	Pick bodies	G389R	M	45	49	4	n.a.	1,170
40 [51, 63]	NFT	R406W	M	63	70	7	3.3	1,121
41 [51, 63]	NFT	R406W	F	58	71	13	3.4	905

Superscript indicates case reference
[uc]Indicates unpublished case
NFT neurofibrillary tangle, *n.a.* APOE genotype or brain weight not available

anti-mouse (Dako 1:200) for 30 min and ABC (Dako) for 30 min. Peroxidase activity was developed with diaminobenzidine/ H_2O_2 solution [10].

The specificity of ET3 has been demonstrated previously in Western blots of recombinant 3R- and 4R-tau [27]. It has also been characterised in immunohistochemical studies of argyrophilic grain disease [13] and other tauopathies [23].

Results

Sporadic FTLD

Semi-quantitative rating data for AT8, ET3 and RD3 immunostaining in the 14 sporadic FTLD cases is given in Table 2.

Cases with Pick bodies

Of the 14 cases with sporadic FTLD, 12 cases (cases #1–12) displayed Pick-type histology. Pick bodies were identified as defined by Kertesz et al. [28], as round or oval, compact intracytoplasmic neuronal inclusions, stained by Bielschowsky but not by Gallyas, tau-immunoreactive and located in dentate fascia, hippocampus and cerebral cortex. Clinically, nine cases (cases #1–7, 9 and 10) showed typical frontotemporal dementia, whereas case #8 had suffered from progressive aphasia and cases #11 and 12 from progressive apraxia. In 11 of these 12 cases (cases #1–4, 6–12), numerous Pick bodies were widespread within frontal and temporal cortex, chiefly in layers two and four and within dentate gyrus granule cells (Fig. 1a) and pyramidal cells of the